Object Removal in Gradient Domain of Cone-Beam CT Projections

Bastian Bier, Martin Berger, Jennifer Maier, Mathias Unberath, Scott Hsieh, Serena Bonaretti, Rebecca Fahrig, Marc E. Levenston, Garry E. Gold, and Andreas Maier

***Abstract*—We propose a method to reduce streak artifacts in cone-beam CT reconstructions that arise from the edges of dense objects outside the 3D field-of-view. To this end, ramp filtering is decomposed into a derivative- and a Hilbert transform step. This allows for spectral inpainting directly in gradient domain, such that only contributions of sharp edges are removed. We applied our approach to weight-bearing knee imaging data, where plastic pipes outside the field-of-view introduce notable streak artifacts. Streak artifacts in the reconstructions are reduced and on semi-simulated data the correlation coefficient could be improved from 0.88 to 0.99. The method is applicable for arbitrary object shapes and can be easily integrated into existing FDK reconstruction algorithms.**

I. Introduction

C-ARM cone-beam computed tomography (CBCT) systems offer an increasing variety of applications, especially due to their high flexibility and their large field-of-view (FOV). Yet, in many cases objects are either truncated or located outside the FOV. Consequently, these objects appear only in a subset of the acquired projections and are not sufficiently sampled, which results in view aliasing and truncation artifacts. The resulting streaking in the reconstruction decreases the diagnostic value of the images. Streaking is more severe if the causing objects have a high attenuation or sharp edges. Common approaches to reduce streak artifacts can be found in metal artifact reduction [1] or view-alias alleviation techniques [2]. Metal artifact reduction techniques often work iteratively or need an initial reconstruction of the object, which is imperative if it is located outside the FOV. View-aliasing artifacts are often compensated for by using algebraic reconstruction techniques, which are computationally expensive. A popular approach seeks to remove patterns from the projections that cause streak artifacts during reconstruction. If the target structures are small, they can usually be removed from the projection images directly via image inpainting [3]. If, however, the structures are large, inpainting in projection domain directly is imperative due to the extensive intensity profile of the object in the projections. The edges of the object, however, are local and the main cause for streaking artifacts. We propose to remove streaking artifact by spectral inpainting in the gradient domain, by decomposing the ramp filter into a derivative and a Hilbert transform [4]. This is beneficial, since the high frequency artifacts in the edge region appear locally in the gradient image, whereas they are smeared into neighboring regions in the ramp filtered image.

B. Bier, M. Berger, J. Maier, M. Unberath, and A. Maier are with the Department of Computer Science, Pattern Recognition Lab, Friedrich-Alexander-University Erlangen-Nuremberg, Erlangen, Germany..

S. Bonaretti, S. Hsieh, R. Fahrig, M. Levenston and G. Gold are with the Stanford University.

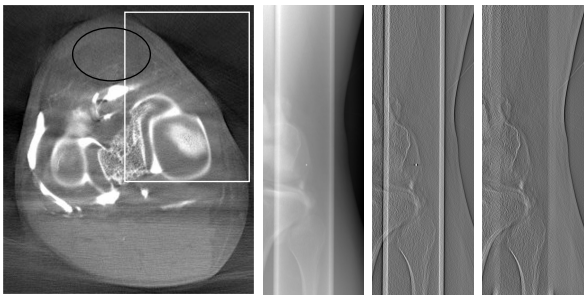

(a) Ground truth reconstruction with marked ROIs. (b) (c) (d)

Fig. 1: Figure 1a shows a slice through the knee joint of a supine scan. Figure 1b shows the raw projection data. Figure 1c and 1d show ramp filtered versions of 1b without and with the proposed object removal.

II. Materials and Methods

Data: To test our algorithm, we used data from weight-bearing and supine knee scans with the same scanning parameters as in [5]. In the weight-bearing scans, two large objects of a stabilization device corrupt a subset of the projections, introducing disturbing streak artifacts. We evaluate our approach on semi-simulated [6], as well as on real data. For the semi-simulated data digitally reconstructed radiographs of the same device are added to a supine scan of the knees, which enables quantitative assessment. The simulated object is a pipe, which is placed vertically over the entire projection.

Reconstruction: The reconstruction is done with the standard FBP pipeline for CBCT data, except that we decomposed the ramp filter into a derivative and the Hilbert-Transform. This allows us to apply the correction algorithm in gradient domain without introducing any other alterations to the reconstruction algorithm.

Mask Creation: A mask M is defined, which covers the object outline in the projections. In these regions, the inpainting will take place. To this end, we define our simulated object in 3D and forward project it such that it aligns with the object in the real data acquisition. The mask M is then extracted from synthetically generated projection images. Since only high variations of the object are responsible for the artifacts,

see Figure 1c in case of the pipe, we define M to segment regions with high gradient magnitude in the projection images. Thus, only the edge region of the object has to be inpainted.

Inpainting: The masked areas are now considered corrupted in the input image I. This area is restored after the computation of the first derivative using spectral interpolation as proposed in [7], yielding the inpainted image G. Interpolation in gradient domain is beneficial over an interpolation of absorption values or after ramp filtering. The first derivative is, compared to the ramp filter, a local operator that preserves the locality of the object boundaries allowing for a precise determination of M without smearing the artifact in a larger area. Thus, the area to be interpolated is smaller and the inner part of the object is unaffected.

High Frequency Recovery: Some important anatomical structures are still visible behind the disturbed area, but are mainly filled with low frequent information in the inpainted image G. We perform a method similar to the one presented in [8], where part of the structures are regained from the subtraction image $S = I - G$. Therefore, S is blurred and subtracted from itself. The resulting residual image contains high frequency information and is added to the inpainted image G. An example projection without and with the proposed correction step is shown in Figure 1c and 1d, respectively. Note that in the center of the shown projections, a fiducial marker is removed, using the approach described in [3].

III. Results

For the semi-simulated data, zoomed regions of a reconstruction slice are shown in Figure 2. Corresponding error measures are shown in Table I. The ROIs for the zoomed region (rectangle) and the error computation (ellipse) are shown in Figure 1a. In Figure 2, we show reconstruction results of the ground truth supine scan, a result containing the simulated pipe, a correction image using the inpainting in projection domain, and our new proposed method. One can see that the proposed method efficiently removes most of the streaks, which are present and indicated in Figure 2b. The calculated error metrics support this observation, where we achieve an improvement of the Cross Correlation (CC) from 0.88 to 0.99, as well as in the Structural Similarity (SSIM) [9] from 0.89 to 0.99. Axial and coronal slices of reconstructions of a standing acquisition with two real pipes outside the FOV are shown in Figure 3. In the original, uncorrected images shown in Figure 3a and 3d the streak artifacts are clearly visible. In the corrected reconstructions, most of the artifacts are removed. The difference images, presented in Figure 3c and 3f, clearly show the removed artifact patterns.

IV. Discussion and Conclusion

We presented a new approach to remove streak artifacts in CBCT reconstructions by inpainting the streak causing areas in the gradient images of the projections. A challenging step is the identification of the corrupted area. In our case, use of prior knowledge was already rewarding, yet, a more sophisticated object detection would increase the usability of the method. Further, the ramp filter could also be decomposed as presented in [10], where the filtering and inpainting could be performed in the image after the second derivative. Due to the removal of some parts in the projections, some mass in the reconstruction result is getting lost, which results in a slight low frequency bias introduced into the reconstructions.

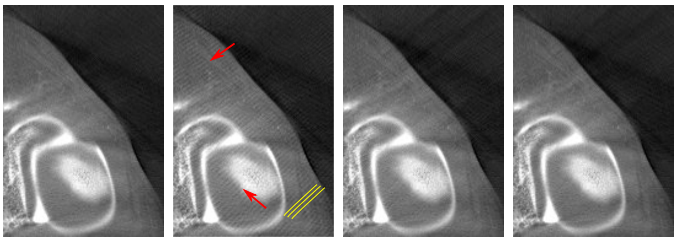

(a) (b) (c) (d)

Fig. 2: Reconstructed regions of the semi-simulated data: (a) ground truth of a supine scan, (b) corrupted, (c) corrected in the line integral domain, (d) correction in gradient domain.

(a) Corrupted. (b) Corrected. (c) Difference Image.

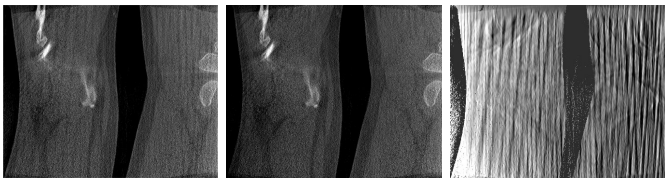

(d) Corrupted. (e) Corrected. (f) Difference Image.

Fig. 3: Reconstruction results of the real data.

TABLE I: CC and SSIM of the ROI shown in Figure 1a.

	CC	SSIM
Corrupted	0.88	0.89
Corrected in line integral domain	0.96	0.97
Proposed method	0.99	0.99

REFERENCES

[1] M. Abdoli *et al.*, "Metal artifact reduction strategies for improved attenuation correction in hybrid PET/CT imaging," *Medical Physics*, vol. 39, no. 6, p. 3343, 2012.

[2] R. R. Galigekere *et al.*, "Techniques to alleviate the effects of view aliasing artifacts in computed tomography." *Medical physics*, vol. 26, no. 6, pp. 896–904, 1999.

[3] M. Berger *et al.*, "Automatic Removal of Externally Attached Fiducial Markers in Cone Beam C-arm CT," *Bildverarbeitung für die Medizin 2014*, pp. 168–173, 2014.

[4] G. L. Zeng, *Medical image reconstruction: A conceptual tutorial*. Springer, 2010.

[5] J.-H. Choi *et al.*, "Fiducial marker-based correction for involuntary motion in weight-bearing C-arm CT scanning of knees. II. Experiment," *Medical Physics*, vol. 41, no. 6, p. 061902, 2014.

[6] A. Maier *et al.*, "Fast simulation of x-ray projections of spline-based surfaces using an append buffer." *Phys. Med. Biol.*, vol. 57, no. 19, pp. 6193–210, 2012.

[7] T. Aach and V. H. Metzler, "Defect interpolation in digital radiography: how object-oriented transform coding helps," in *SPIE*, vol. 4322, 2001, pp. 824–835.

[8] C. Schwemmer *et al.*, "High-Density Object Removal from Projection Images using Low-Frequency-Based Object Masking," in *Bildverarbeitung für die Medizin 2010*, Berlin, 2010, pp. 365–369.

[9] Z. Wang *et al.*, "Image quality assessment: From error visibility to structural similarity," *IEEE Transactions on Image Processing*, vol. 13, no. 4, pp. 600–612, 2004.

[10] F. Dennerlein and A. Maier, "Region-of-interest reconstruction on medical C-arms with the ATRACT algorithm," in *Proc. SPIE Medical Imaging 2012*, vol. 8313, 2012, pp. 83 131B–83 131B–9.